Mon. Not. R. astr. Soc. (1982) **198**, 1033–1052

Background radiation fields as a probe of the large-scale matter distribution in the Universe

N. Kaiser *Institute of Astronomy, Madingley Road, Cambridge CB3 0HA*

Received 1981 July 16; in original form 1981 June 15

Summary. A 'Swiss Cheese' model is used to calculate to order of magnitude the temperature fluctuation of the CMB in a lumpy universe. The calculations are valid in a Friedmann background of aribtrary Ω provided that matter has been dominant since the photons were last scattered. The inhomogeneities may be larger than the curvature scale, as is required to deal with fluctuations on a large angular scale in a low-density universe. We combine this model with observational limits on the fluctuations in the CMB to yield an upper limit to the present spectrum of inhomogeneities. The absence of any quadrupole anisotropy $\gtrsim 3 \times 10^{-4}$ sets a limit on the amplitude of lumps on scales very much greater than the present horizon. We see that, as shown by Peebles, for $\Omega = 1$ and a simple (Poisson) model the predicted $\Delta T/T(\theta)$ is in remarkable accord with the recent measurements of quadrupole and 6° anisotropy. For a low-density model the predicted $\Delta T/T(\theta)$ for large angles is markedly different. We briefly consider the limits on inhomogeneity from the isotropy of the X-ray background and find them to be consistent with the microwave limits. We note that, if there is no X-ray source evolution, then failure to detect a dipole anisotropy in the X-rays at the ~ 1/3 per cent level would favour a high-density universe.

1 Introduction

If the matter distribution of the Universe is slightly inhomogeneous on very large scales then we would expect to observe anisotropy in the background radiation fields. In this paper we shall consider the constraints on the lumpiness of the Universe that are imposed by the observed degree of isotropy of the radiation fields.

The cosmic microwave background radiation (CMB) has a thermal spectrum at a temperature of $T_0 = 2.7 \pm 0.1$ K. Scans of the sky reveal this to be highly isotropic, although the existence of a dipole anisotropy, $T = T_0(1 + \epsilon \cos\theta)$ with $\Delta T/T = \epsilon \simeq 10^{-3}$, is well established (e.g. Smoot, Gorenstein & Muller 1977). This relative temperature measurement can be made with much greater precision than the absolute measurement of T_0. Boughn, Cheng & Wilkinson (1981) claim to have discovered a quadrupole anisotropy of amplitude $\sim 10^{-4}$, while Fabbri *et al.* (1980, 1981) report a 'quadrupole like anisotropy' of amplitude $\sim 3 \times 10^{-4}$ and a fluctuation on a 6° scale of amplitude 3×10^{-5}. Otherwise we have upper limits on $\Delta T/T$ of $\sim 3 \times 10^{-4}$ from Smoot (1980).

There is no need to invoke a cosmology which is inhomogeneous on a large scale to explain the observed dipole fluctuation since this is precisely the pattern observed by a radio astronomer who has a peculiar velocity $V = \epsilon C \sim 300\,\mathrm{km\,s^{-1}}$ relative to a frame in which the radiation appears isotropic. Such a peculiar velocity could easily have been produced by our association with some nearby, relatively small structure, e.g. the Local Supercluster (White 1980). Other anisotropies must be intrinsic to the radiation field, provided that they are not due to local emission.

The effect of large-scale lumps on the CMB has been investigated by various authors. One approach is to apply linearized gravity theory to perturb the cosmological model. Sachs & Wolfe (1967) perturb the Einstein field equations about the Einstein–de Sitter solution. They decompose the general perturbation into spatial Fourier components and find a solution with terms that they identify as gravitational waves, rotation (eddy) fluctuations and density fluctuations. For the latter they integrate the null geodesics (light rays) back to the cosmic photosphere and find a temperature fluctuation mainly due to lumps on the photosphere. For a small-amplitude plane-wave fluctuation of wavelength λ they find

$$\frac{\Delta T}{T} \sim \left(\frac{\lambda}{\lambda_{\mathrm{H}}}\right)^2 \left(\frac{\Delta\rho}{\rho}\right)_0, \tag{1}$$

where $(\Delta\rho/\rho)_0$ is the present amplitude (density contrast and λ_{H} is the Hubble radius $= c/H_0$. This approximation breaks down for $\lambda/\lambda_{\mathrm{H}} \gtrsim 1$. Anile & Motta (1976) have generalized the Sachs & Wolfe result to a general Friedmann background but only for lumps smaller than the curvature scale. A lump the size of the curvature radius sitting on our horizon subtends an angle

$$\theta = \frac{\Omega_0}{2\sqrt{1-\Omega_0}} \qquad (\sim 0.1 \text{ for } \Omega_0 = 0.2).$$

The Anile & Motta result should be valid to describe fluctuations only for smaller scales.

By essentially the same approach (still for the special case of Einstein–de Sitter), the effect of density perturbations in the long wavelength $\lambda \gg \lambda_{\mathrm{H}}$ limit is found by Grishchuk & Zel'dovich (1978) to be

$$\frac{\Delta T}{T} \sim \left(\frac{\Delta\rho}{\rho}\right)_0. \tag{2}$$

An alternative approach, and the one we will follow, is to use an exact non-linear solution due to Einstein & Straus (1945): the 'Swiss Cheese' universe containing rather idealized spherical lumps in an otherwise homogeneous background. Little benefit derives here from the non-linear nature of the solution, since the lumps we treat are of small amplitude. The advantage of this model is that one can treat perturbations on scales larger than the curvature radius that may be responsible for large angular scale fluctuations on the CMB. Kantowski (1969) has used this model to correct the luminosity-redshift relation for the presence of inhomogeneities. Rees & Sciama (1968) and Dyer (1976) use the Swiss Cheese model to calculate the temperature profile observed for a lump between us and the photosphere. In the linear regime this effect is found to be much smaller than the Sachs & Wolfe effect, going like

$$\frac{\Delta T}{T} \propto \left(\frac{\lambda}{\lambda_{\mathrm{H}}}\right)^3 \left(\frac{\Delta\rho}{\rho}\right)_0. \tag{3}$$

While there is no need for a large lump to produce the dipole fluctuation, we cannot exclude large lumps as a possible cause, and so the dipole measurement still provides a constraint on the amplitude of large-scale lumps. An observer at the edge of a lump will see (Peebles 1976)

$$\frac{\Delta T}{T} \simeq \Omega_0 \left(\frac{\lambda}{\lambda_{\mathrm{H}}}\right) \left(\frac{\Delta \rho}{\rho}\right)_0 f(\Omega_0), \tag{4}$$

where Ω_0 is the density parameter. f is a slowly decreasing function of Ω_0.

The X-ray background, observed over a wide range of energies, can also provide a probe of large-scale density inhomogeneities. Satellite observations reveal this radiation to be isotropic to within about 1/2 per cent. If we assume that the X-ray source density is enhanced in regions of excess matter density then, as we look towards a lump, we will see an excess intensity. In fact we see the integrated density out to a distance of the order of Hubble radius. In addition to this direct observation, lumps may betray themselves through the peculiar velocities that they induce in us and in the source region. These effects have been investigated by Fabian & Warwick (1979).

The strongest constraint on large-scale inhomogeneities comes from the Sachs & Wolfe effect, but the requirement that the radius of curvature of the background be much larger than the scale of the inhomogeneity means that one effectively has an Einstein–de Sitter background. We will use a Swiss Cheese model to determine these effects for arbitrarily large lumps. In the following section we construct a Swiss Cheese universe. In Section 3 we determine the appearance of the CMB in such a universe. In Section 4 we consider X-ray anisotropies and in Section 5 we combine the theory with observational limits on the amplitude of large-scale lumps.

2 A Swiss Cheese universe

In this section we set up the Swiss Cheese universe, an exact inhomogeneous solution to the field equations, which contains one or more spherical lumps. This is done by exploiting the spherical symmetry of the system and patching together parts of spherically symmetric solutions that have already been obtained, namely the spacetimes of Friedmann and of Schwarzschild. First we introduce the Friedmann universe which will constitute the background; this serves to introduce the notation. Then we construct a lump, examine its rate of growth and calculate the redshift for a photon entering or emerging from the lump.

2.1 THE FRIEDMANN (DUST) SOLUTION

This is a universe containing a uniform pressure-free fluid. Choosing units in which c and G have unit numerical value, the line element, written in comoving spatial coordinates, is

$$ds^2 = -d\tau^2 + R^2(\tau)[d\omega^2 + S_k^2(\omega)\, d\sigma^2] \tag{5}$$

where τ = proper time, $d\sigma^2 = d\theta^2 + \sin^2\theta\, d\phi^2$ is an element of solid angle, θ, ϕ are polar angles, ω is a dimensionless radial coordinate and

$$S_k(\omega) \equiv \begin{cases} \sin\omega \\ \omega \\ \sinh\omega \end{cases} \text{for curvature constant } k = \begin{cases} +1 \\ 0 \\ -1 \end{cases}$$

$R(\tau)$ is the scale factor, whose evolution is determined by the Friedmann equation

$$\left(\frac{dR}{d\tau}\right)^2 = \frac{2M}{R} - k \tag{6}$$

where $M \equiv \frac{4}{3}\pi\rho R^3$ = constant and ρ is the matter density. This equation yields a parametric solution

$$\left.\begin{aligned} R &= Mk[1 - C_k(\eta)] \\ \tau &= Mk[\eta - S_k(\eta)] \end{aligned}\right\} \text{ where } C_k(\omega) = \begin{cases} \cos\omega \\ 1 \\ \cosh\omega \end{cases}. \tag{7}$$

At early times, $\eta \ll 1$, all models have $R \propto \tau^{2/3}$. At sufficiently late times, $\eta \gg 1$, gravity loses out in a $k = -1$ model, and we have $R \propto \tau$, i.e. geometric expansion.

The different Friedmann histories are distinguished by M (and k) so the background in which we live is specified by M and τ_0 (or η_0), the time since the Big Bang. More convenient to measure are the Hubble parameter $H \equiv (dR/d\tau)R^{-1} = \dot{R}R^{-1}$ and the density parameter $\Omega \equiv \rho/\rho_{\text{crit}} = 8\pi\rho/(3H^2)$. Observations suggest $0.02 < \Omega_0 \lesssim 1$. A subscript 0 denotes a measurement made at the present epoch.

$$\frac{1}{\Omega} - 1 = \frac{R\dot{R}^2}{2M} - 1 = -\frac{1}{2}[1 - C_k(\eta)] = -\frac{kR}{2M} \tag{8}$$

relates η and Ω. From equation (7) we see that $d\tau = R(\tau)\,d\eta$, so radial photons (null $\Rightarrow ds^2 = 0$) have $d\eta/d\omega = \pm 1$. The particle horizon size is $\omega_{\text{H}} = \eta$. The redshift measured by comoving observers is

$$1 + z \equiv \lambda_{\text{obs}}/\lambda_{\text{em}} = R_{\text{obs}}/R_{\text{em}}, \tag{9}$$

so a freely moving photon has a wavelength proportional to the scale factor. Each photon loses energy (as measured by the fundamental observers it is passing) as time goes on, so there will have been an epoch in the past, τ_{eq}, before which the radiation will have dominated the energy density – in the standard hot Big Bang model $\tau_{\text{eq}} < \tau_{\text{rec}}$, the time from which we begin tracing null rays if $\Omega_0 \gtrsim 0.2\,h^{-2}$, in which case our assumption of a matter-dominated universe is justified.

Let us obtain the relation $\omega(z)$ giving the dimensionless radial coordinate of an object observed at a redshift z. By (8),

$$k\frac{(1 - 1/\Omega_0)}{1 + z} = k(1 - 1/\Omega) = \frac{k}{2}[1 - C_k(\eta)] = S_k^2(\eta/2),$$

then

$$\omega(z) = \eta_0 - \eta_{\text{em}} = 2\left[S_k^{-1}\sqrt{k(1 - 1/\Omega_0)} - S_k^{-1}\sqrt{\frac{k(1 - 1/\Omega_0)}{1 + z}}\right] \tag{10}$$

Since we shall be dealing with low-amplitude lumps whose interiors expand at almost the same rate as the background, it is useful to answer the question: how does the angular size θ subtended by a comoving sphere depend on its distance from us? If we observe a sphere of radius ω_{s} at a distance ω by photons emitted at τ_{em} then, setting the origin at the centre of the lump, the proper diameter is (by equation 5) $l = 2R(\tau_{\text{em}})\omega_{\text{s}}$. Setting the origin at our position gives $l = R(\tau_{\text{em}})\,2\theta S_k(\omega)$ and so

$$\theta = \frac{\omega_{\text{s}}}{S_k(\omega)}. \tag{11}$$

This is the angular scale on which effects from lumps, size ω_{s}, at a distance ω will show up.

In the standard Big Bang model, the universe is transparent back to the epoch of recombination ($z_{\text{rec}} \simeq 1400$, $T_{\text{rec}} \simeq 1400 \times \tau_0 \simeq 4000\,\text{K}$) before which Thomson scattering couples the matter and radiation. From equation (10) we see that $\omega(z = 1400)$ is only slightly less than the horizon size now, $\omega(\infty)$. From (10) the horizon size at recombination is

$$\omega_{H_{\rm rec}} = 2S_k^{-1}\sqrt{\frac{k(1-1/\Omega_0)}{1+z_{\rm rec}}}.$$

The angular size of a lump the size of the horizon at recombination on our recombination horizon is

$$\theta = \frac{\omega_{H_{\rm rec}}}{S_k(\omega_{H_0})} = \frac{2S_k^{-1}\sqrt{k(1-1/\Omega_0)/1+z_{\rm rec}}}{S_k[2S_k^{-1}\sqrt{k(1-1/\Omega_0)}]} \simeq \sqrt{\frac{\Omega_0}{1+z_{\rm rec}}} \qquad \text{if } 1+z_{\rm rec} \gg k(1-1/\Omega_0)$$

and is small, though if reheating takes place the photosphere could be at a redshift as low as $z \sim 10$ and the angular size would be correspondingly increased.

Although the cosmic photosphere will have a finite width and so will tend to smear out the effect of lumps on the cosmic photosphere which are smaller than this width, we may safely take it to be a sharp transition since we are mainly concerned with lumps a good deal larger than the horizon size at recombination.

Our task will be to introduce lumps into this background and, in the microwave treatment, trace null geodesics back to the cosmic photosphere, evaluating the observed radiation temperature and comparing it with the results obtained in an unperturbed universe – or equivalently that observed in a direction away from the lump(s). This raises the problem that, for lumps which are on the cosmic photosphere (so that photons from that direction were last scattered within the lump), we need to know the thermal nature of the lump, since this in part determines the distance from us of that region of the photosphere which is within the lump. In a Friedmann universe the specific entropy is constant (in the absence of irreversible reactions) and is equal to the ratio $\mathfrak{S} = n_\gamma/n_{\rm B}$ = number of photons per baryon, which is observed to be $\sim 10^8$ in our Universe. As we shall see, the interior of one of our lumps resembles a portion of another Friedmann universe – with different M – and, at least while it is larger than the horizon size so photons cannot escape, $n_\gamma/n_{\rm B}$ will be a constant therein, though not necessarily the same value as in the background. In our model the entropy per baryon is an unspecified function of M – setting this to be a constant yields isentropic perturbations.

2.2 THE DYNAMICS OF A LUMP

Within the homogeneous background we may carve out a sphere of dust and replace it with a smaller expanding dust sphere having the same gravitational mass as the excised sphere. The interior will behave like a finite sphere in another Friedmann universe (with different M), the exterior is unperturbed and by Birkhoff's theorem the spherically symmetric vacuum spacetime in the gap is Schwarzschild. We may repeat this procedure at various points until we have a universe populated with lumps of various sizes: we may have lumps within lumps, but the vacuum shells of different lumps may never intersect. In addition, the initial conditions chosen for the lump must exclude shell crossing for an individual lump at least over the range of time with which we are concerned. This 'Swiss Cheese' universe is an exact solution to the field equations which represents a rather idealized inhomogeneous cosmology. It is, however, a universe for which we can perform the prescribed ray-tracing calculations, the general form of the results of which we might expect to obtain in a realistic lumpy universe.

Let A, B be observers on the outer and inner edges of the vacuum shell with a radial separation. Observers such as A, B may be considered to be comoving observers in their respective Friedmann universes or, equivalently, as test particles ejected from the origin following time-like geodesics in Schwarzschild geometry. Naturally enough, an interface with an open/closed Friedmann region requires an unbound/bound orbit. If A and B emerge from the same event but with different total energies (E is the specific energy attributed to a test particle by an observer at rest at infinity in the asymptotically flat Schwarzschild 4-geometry) then this, we shall see, produces a growing perturbation. One can also treat the case of the delayed core where there is an interval between the ejection of A and that of B (non-simultaneity of Big Bang time), and this produces the decaying mode.

Writing the line element for the Schwarzschild geometry in the usual $x^i = (t, r, \theta, \phi)$ coordinates

$$ds^2 = g_{ij}\, dx^i\, dx^j = -\left(1 - \frac{2m}{r}\right) dt^2 + \left(1 - \frac{2m}{r}\right)^{-1} dr^2 + r^2\, d\sigma^2, \tag{12}$$

we see that $k^i \equiv (1, 0, 0, 0)$ is a Killing vector which provides us with a constant of the motion $k \cdot U = U_0 = -E$ say, where U is the 4-velocity of the test particle. From this, and the condition $U \cdot U = -1$ for time-like geodesics, we get the equations of motion

$$E^2 - V^2 = 1 - \frac{2m}{r}, \tag{13}$$

where

$$V \equiv \frac{dr}{d\tau},$$

and

$$\frac{dt}{d\tau} = \frac{E}{(1 - 2m/r)}. \tag{14}$$

(13) is essentially the Friedmann (Newton) equation and yields a parametric solution

$$\left.\begin{aligned} r &= \frac{kM}{S^2}\,[1 - C_k(\eta')] \\ \tau &= \frac{km}{S^3}\,[\eta' - S_k(\eta')] \end{aligned}\right\} \tag{15}$$

where

$$S \equiv \sqrt{k(1 - E^2)}.$$

We see from (15) that

$$V = \frac{S S_k(\eta')}{k[1 - C_k(\eta')]}.$$

We now have to match together the two 4-geometries at their interface. This matching is established by demanding that, if we measure the area of an element of the interface in which A or B lies, the result obtained should be independent of the metric used. Then equations (5) and (12) imply the relationship between Schwarzschild and Friedmann radial coordinates $r = R S_k(\omega)$. Comparing the solutions (7) and (15) we find $MS^2 S_k(\omega) = m$, $\eta' = \eta$. A further requirement is that the proper time elapsed since the Big Bang as measured by an observer at an interface be similarly invariant. Then equations (7) and (15) imply

$m = MS^3$, so $S = S_k(\omega)$ and $m = \frac{4}{3}\pi\rho r^3$. The Schwarzschild solution for mass m matches smoothly on to a Friedmann region with parameter M at a comoving radius ω via $m = MS_k^3(\omega)$. The specific energy of the test particle is given by $E = C_k(\omega)$. Equation (15) provides $r(\tau)$ parametrically. We can also integrate equation (14) to get the full solution for the orbits:

$$r(S,\eta) = \frac{km}{S^2}[1 - C_k(\eta)],$$

$$t(S,\eta) = \frac{kmE}{S^3}[(1+2kS^2)\eta - S_k(\eta)] + 2m \ln \left| \frac{S_k(\omega - \eta/2)}{S_k(\omega + \eta/2)} \right|, \tag{16}$$

$$\tau(S,\eta) = \frac{km}{S^3}[\eta - S_k(\eta)],$$

where S specifies the orbit and η is a parameter along the orbit.

A lump of size ω comes within the horizon when $\eta = \omega$. At that epoch

$$r = \frac{km[1 - C_k(\omega)]}{S_k^2(\omega)} = m\frac{[1 - C_k(\omega)]}{[1 - C_k^2(\omega)]} = \frac{m}{C_k(\omega) + 1},$$

whereas that lump is the size of its Schwarzschild radius, $r = 2m$, when $\eta = 2\omega$ (slightly later). The non-relativistic approximation will only be valid after that epoch, i.e. when the lump has come well within the horizon.

2.3 GROWTH OF THE PERTURBATIONS

Let us measure ρ (and hence $\Delta\rho/\rho$) on the space-like hypersurfaces that are orthogonal to the 4-velocities of our fundamental observers. These are hypersurfaces of constant τ. Although this choice of gauge is arbitrary, it is a fairly natural choice which coincides with the usual unambiguously defined simultaneity for non-relativistic calculations. We have $m = \frac{4}{3}\pi\rho r^3 = \text{constant}$ (across the gap), so the fractional density change is $\Delta\rho/\rho = -3(\Delta r/r)$. Let us calculate $\Delta r/r$: taking $r(S,\eta)$, $t(S,\eta)$ from equations (16), we have

$$\Delta r = \frac{\partial r}{\partial S}\Delta S + \frac{\partial r}{\partial \eta}\Delta\eta, \qquad \Delta t = \frac{\partial t}{\partial S}\Delta S + \frac{\partial t}{\partial \eta}\Delta\eta.$$

But the separation $S^i \equiv (\Delta t, \Delta r, 0, 0)$ has $U \cdot S = 0$, and eliminating $\Delta\eta$ gives

$$\frac{\Delta r}{r} = \frac{S}{r}\frac{\Delta S}{S}\left[\frac{E^2(\partial r/\partial S) - EV(E^2 - V^2)(\partial t/\partial S)}{E^2 - V^2}\right].$$

From (16) we obtain

$$\frac{\partial r}{\partial S} = -\frac{2r}{S}, \qquad \frac{\partial t}{\partial S} = \frac{-1}{ES}\left[3\tau + \frac{2Vr}{E^2 - V^2}\right],$$

and so

$$\frac{\Delta r}{r} = \frac{\Delta S}{S}\left[\frac{3V\tau}{r} - 2\right] = \frac{\Delta S}{S}\left[\frac{3kS_k(\eta)[\eta - S_k(\eta)]}{[1 - C_k(\eta)]^2} - 2\right]. \tag{17}$$

Note that, for $\eta \ll 1$,

$$\frac{\Delta r}{r} \simeq \frac{\eta^2}{10}\left(\frac{-k\Delta S}{S}\right)$$

while, for $\eta \gg 1$, $k=-1$,

$$\frac{\Delta r}{r} \simeq \frac{\Delta S}{S}.$$

These lumps grow with $\Delta\rho/\rho \propto \tau^{2/3}$ until $\eta \simeq 1$ whereafter, in an open model, they quickly reach their 'frozen-in' value $\Delta\rho/\rho = 3(\Delta S/S)$. $\Delta \equiv |\Delta S/S|$ is clearly a gauge-invariant amplitude.

In the next section we find that we can express the extra redshift due to the presence of the lump in terms of $(\Delta r/r)_\pm$ and $z_\pm$. Here $z_\pm$ is the redshift incurred crossing the gap for a radial $\binom{\text{outward}}{\text{inward}}$ photon and $(\Delta r/r)_\pm$ is the corresponding null separation.

Since $(\Delta t, \Delta r, 0, 0) \propto P^i$, the 4-momentum of the photon, $P\cdot P = 0 \Rightarrow \Delta r = \pm(1-2m/r)\Delta t$, with which we can eliminate $\Delta\eta$ from

$$\Delta r = \frac{\partial r}{\partial S}\Delta S + \frac{\partial r}{\partial \eta}\Delta\eta$$

to obtain

$$\left(\frac{\Delta r}{r}\right)_\pm = \pm k\left(1 \pm \frac{V}{E}\right)\left(2 - \frac{3V\tau}{r}\right)\Delta \equiv \pm\left(1 \pm \frac{V}{E}\right)D_k(\eta)\Delta, \tag{18}$$

where

$$D_k(\eta) \equiv k[\![2 - 3kS_k(\eta)\,[\eta - S_k(\eta)]/[1 - C_k(\eta)]^2]\!].$$

To get $z_\pm$, we use the result that a photon with 4-momentum P is observed to have a frequency $\nu \propto U\cdot P$, where U is the 4-velocity of the observer. $P\cdot P = 0$ and $k\cdot P =$ constant $\Rightarrow P_i \propto [-1, \pm(1-2m/r)^{-1}, 0, 0]$ and the equations of motion provide u^i. Combining these gives

$$\nu \propto \frac{1}{E+V} \propto \frac{1}{\lambda},$$

so

$$\lambda = \lambda_0(E \pm V) = \lambda(r, S),$$

and

$$z_\pm = \frac{\Delta\lambda}{\lambda}$$

gives

$$z_\pm = \frac{S^2}{EV}\left[1 + \frac{k}{2}\left(\frac{3V\tau}{r} - 2\right)\left(\frac{V^2}{S^2} - 1\right)\right]\Delta \equiv \frac{S}{E}A_k(\eta)\Delta. \tag{19}$$

The redshift depends on the size of the lump as S/E and on the epoch at which the photon crosses the gap, but not on the direction of travel. If $\eta \ll 1$ then $A(\eta) \sim \eta$, and if $\eta \gtrsim 1$ then $A(\eta) \simeq 1$.

3 The CMB in a Swiss Cheese universe

Having set up this exact solution for a single spherical lump we can construct a universe populated with lumps of various sizes. Although this picture is highly idealized, it does share the major feature of a realistic lumpy universe; that is, regions of overdensity interspersed with regions of underdensity, and so we can reasonably expect to see the same spectrum of angular fluctuations in the CMB in a real universe as in a Swiss Cheese universe populated with lumps of a suitable amplitude and scale.

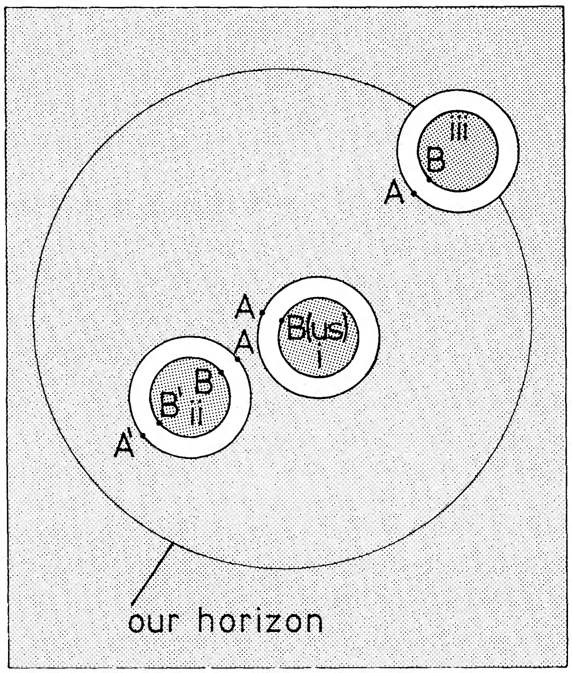

Figure 1. Schematic diagram of a Swiss Cheese universe containing three lumps: (i) the local lump, (ii) a transparent lump between us and the photosphere, (iii) a lump on the last scattering surface.

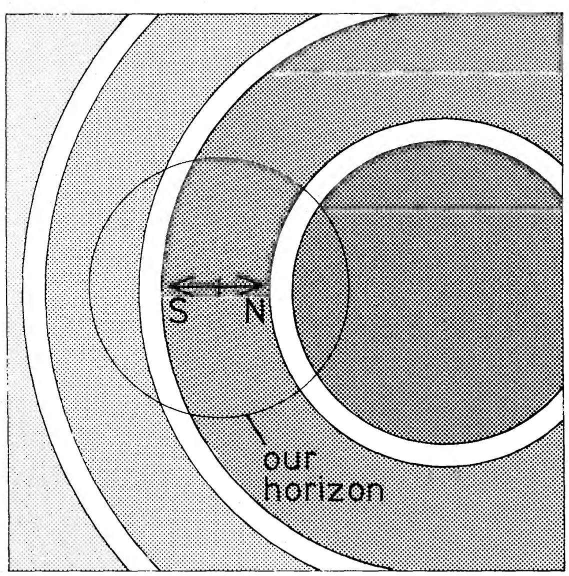

Figure 2. Part of a very large lump. We calculate the temperature observed in directions towards the poles and in the equatorial plane.

We shall calculate the effect of one lump at a time, treating separately the case of:

(1) A local lump (inside the present horizon) of which we happen to be a part.
(2) A transparent lump between us and the photosphere.
(3) A lump on the photosphere. These three cases are shown schematically in Fig. 1.
(4) A lump (larger than the present horizon size) of which we happen to be a part (see Fig. 2).

Though we wish to predict the observed radiation temperature fluctuations we can calculate the redshift and use Liouville's theorem (Misner, Thorne & Wheeler 1973) to show that the radiation, if initially thermal, remains thermal and so the mean temperature fluctuation is just $\langle|\Delta T/T|\rangle = z$ where z is the extra redshift. Since we want an estimate of $\langle|\Delta T/T|\rangle$, we perform the calculation for a photon passing radially through the lump and compare this with the unperturbed case rather than extract the observed temperature profile across the lump.

The lumps have small amplitude $|\Delta S/S| \ll 1$, so all calculations will be to first order in Δ.

3.1 THE NEARBY LUMP

We expect such a lump to induce a 24-hr $(\cos\theta)$ fluctuation through the Compton–Getting effect with

$$\left\langle\left|\frac{\Delta T}{T}\right|\right\rangle \sim V_{\rm p}$$

our peculiar velocity.

For our lumps this effect will be greatest for an observer such as B (see Fig. 1).

Let us calculate the extra redshift $(1+z) \equiv \lambda_{\rm L}/\lambda_{\rm b}$ due to the presence of the lump. Writing $\lambda_{\rm obs}$ = (product of redshifts incurred on the trip) $\times\, \lambda_{\rm em}$ (recombination takes place everywhere at the same $T \Rightarrow \lambda_{\rm em}$ = constant, take $\lambda_{\rm em}$ to be the peak of the spectrum say),

$$1+z = \frac{(\lambda_{\rm L}/\lambda_{\rm B'})(\lambda_{\rm B'}/\lambda_{\rm A'})(\lambda_{\rm A'}/\lambda_{\rm E})}{(\lambda_{\rm b}/\lambda_{\rm A})(\lambda_{\rm A}/\lambda_{\rm E})} = \frac{(r_{\rm A'}/r_{\rm B'})(1+z'_-)}{(r_{\rm A}/r_{\rm B})(1+z_-)}$$

since $\lambda \propto r$ in any Friedmann region. Then

$$z = \left[\left(\frac{\Delta r}{r}\right)_- - z_-\right]_{\eta_0} - \left[\left(\frac{\Delta r}{r}\right)_- - z_-\right]_{\eta_0 - 2\omega}$$

and we see from (18), (19) that

$$\left(\frac{\Delta r}{r}\right)_- - z_- = \left\{-D_k(\eta) + \frac{S}{E}\left[\frac{D_k(\eta)}{2}\left(\frac{3V}{S} - \frac{S}{V}\right)\right]\right\}\Delta$$

so

$$Z/\Delta = -2\omega\frac{dD_k(\eta)}{d\eta} + O(\omega^2).$$

But

$$\left(\frac{\Delta\rho}{\rho}\right)_0 = 3D_k(\eta_0)\Delta,$$

so

$$z = -\left(\frac{\omega}{\omega_{H_0}}\right)\left(\frac{2}{3}\frac{\eta}{D}\frac{dD}{d\eta}\right)_0\left(\frac{\Delta\rho}{\rho}\right)_0 \equiv -\frac{\omega}{\omega_{H_0}} g_1(\Omega_0)\left(\frac{\Delta\rho}{\rho}\right)_0, \tag{20}$$

$$g_1(1) = \frac{4}{3}, \qquad g_1(0.2) \simeq 0.8.$$

In this single-shell model, this is the fluctuation seen by an observer on the very edge of the lump (B). The fluctuation increases linearly with distance from the origin for observers in the interior of the lump. The peculiar velocity is zero for observers outside the vacuum shell – the redshift in that case is much smaller (see next calculation). For a more realistic spherical inhomogeneity (nested shells), an observer will be sensitive to those shells inside which he lies.

Each shell contributes

$$z_{\text{shell}} = -\frac{\omega_{\text{obs}}}{\omega_{\text{shell}}}\frac{\omega_{\text{shell}}}{\omega_{H_0}}\Delta_{\text{shell}}\, g_1(\Omega_0),$$

and

$$z = \Sigma z_{\text{shell}} \simeq \frac{\omega_{\text{obs}}}{\omega_{\text{L}}}\left[\frac{\omega_{\text{L}}}{\omega_{H_0}} g_1(\Omega_0)\left(\frac{\Delta\rho}{\rho}\right)\right],$$

so here too the redshift increases linearly with radius near the origin, going to zero as one enters the background. Averaging over all space to obtain an estimate of the typical effect will introduce a factor ~ the fractional volume occupied by lumps ~ 1/10 say. The limit on $(\Delta\rho/\rho)_0$ with $z = 10^{-3}$ (the observed dipole amplitude) is shown as line 1 in Fig. 3. In the case of the mode that is actually responsible for the observed 24-hr fluctuation, we may well be in a privileged position and so we should take something nearer this maximum effect.

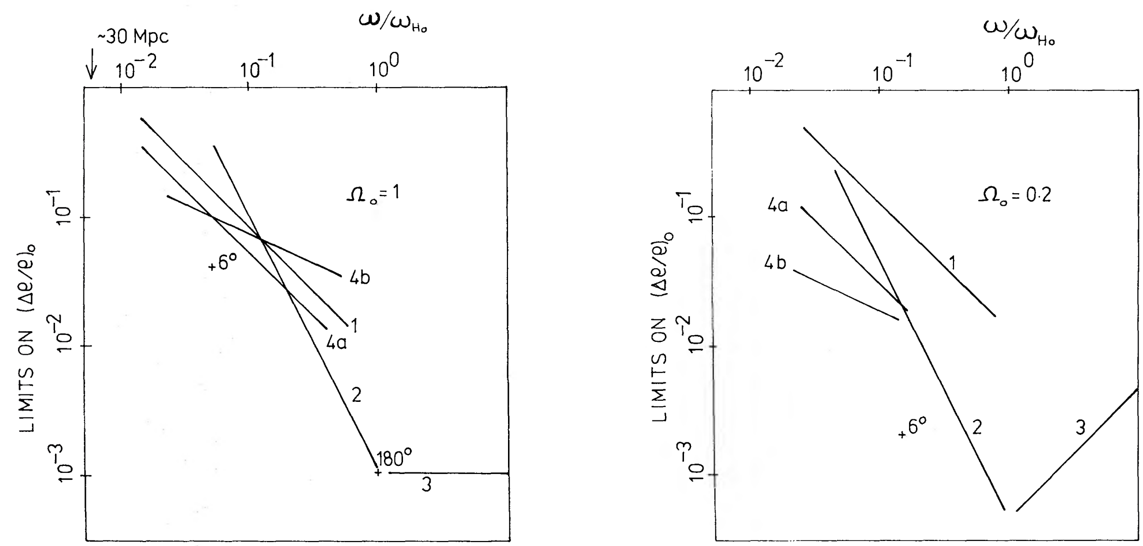

(a) (b)

Figure 3. Upper limits to the present density contrast plotted against size of the lumps for $\Omega_0 = 1$ (a) and for $\Omega_0 = 0.2$ (b). (1) The peculiar velocity effect, assumes $\Delta T/T < 10^{-3}$; (2) lumps on the last scattering surface where I have assumed $\Delta T/T < 3 \times 10^{-4}$; (3) limits to long wavelength modes from the quadrupole limits; (a) X-ray limits – no evolution. (b) X-ray limits assuming evolution – no sources at redshift less than 2. The X-ray limits assume $(\Delta I/I)_X < 10^{-2}$.

3.2 A TRANSPARENT LUMP BETWEEN US AND THE PHOTOSPHERE

The product of redshifts yields

$$(1+z)=\frac{\lambda_L}{\lambda_A}\left(\frac{\lambda_A}{\lambda_B}\right)\frac{\lambda_B}{\lambda_{B'}}\left(\frac{\lambda_{B'}}{\lambda_{A'}}\right)\frac{\lambda_A}{\lambda_E}\left(\frac{\lambda_b}{\lambda_E}\right)^{-1}=\frac{r_B}{r_A}\left(\frac{\lambda_A}{\lambda_B}\right)\frac{r_{A'}}{r_{B'}}\left(\frac{\lambda_{B'}}{\lambda_{A'}}\right),$$

so

$$z=\left[z_+-\left(\frac{\Delta r}{r}\right)_+\right]_\eta+\left[z_--\left(\frac{\Delta r}{r}\right)_-\right]_{\eta-2\omega}.$$

Now

$$z_\pm=\frac{S}{E}A_k(\eta)\Delta,\qquad\left(\frac{\Delta r}{r}\right)_\pm=\pm D\Delta+\frac{S}{E}\frac{V}{S}D\Delta,$$

so, expanding as a Taylor series about η:

$$\frac{z}{2\Delta}=\omega\left[A-\frac{VD}{S}-\dot{D}\right]-\omega^2\frac{d}{d\eta}\left[A-\frac{VD}{S}-\dot{D}\right]$$
$$+\omega^3\left\{\frac{d^2}{d\eta^2}\left[A-\frac{VD}{S}-\dot{D}\right]-\frac{1}{3}\left[A-\frac{VD}{S}-\dddot{D}\right]\right\}+O(\omega^4)$$

where

$$\dot{D}\equiv\frac{dD}{d\eta}.$$

But

$$A-\frac{VD}{S}-\dot{D}=0,$$

so

$$z=\frac{2}{3}\omega^3(\dddot{D}-\dot{D})\Delta$$

or, since

$$\left(\frac{\Delta\rho}{\rho}\right)_0=3D_0\Delta,\qquad\omega_{H_0}=\eta_0,$$

$$z=\left(\frac{\omega}{\omega_{H_0}}\right)^3h(\Omega,\Omega_0)\left(\frac{\Delta\rho}{\rho}\right)_0,$$

where

$$h=\frac{2}{9}\frac{\eta_0^3}{D_0}(\dddot{D}-\dot{D}),$$

and we must evaluate $\dddot{D}-\dot{D}$ as the photon emerges. Thus $\omega\sim(\omega/\omega_{H_0})^3(\Delta\rho/\rho)_0$, with the possible exception of the most distant lumps (that are also outside the horizon at recombination). Here the non-zero term is $\sim(\omega/\omega_{H_0})^2(\Delta\rho/\rho)_0$. This is suggestive, but the ordering in the Taylor series has broken down; 'higher order' terms may contribute at the same order and possibly cancel the 'ω^3' term. We shall see in the next section that lumps on the photosphere have $z \sim (\omega/\omega_{H_0})^2 (\Delta\rho/\rho)_0$ and so we may conclude that transparent lumps have negligible effect.

3.3 A LUMP ON THE PHOTOSPHERE

The product of the redshifts yields

$$(1+z) \equiv \frac{\lambda^1}{\lambda_0} = \frac{\lambda^1}{\lambda_A}\left(\frac{\lambda_A}{\lambda_B}\right)\frac{\lambda_B}{\lambda^1_{em}}\lambda^1_{em}\left(\frac{\lambda_0}{\lambda_{em}}\lambda_{em}\right)^{-1} = \frac{(r_{A_0}/r_A)(\lambda_A/\lambda_B)(r_B/r_{B_{rec}})}{(r_{A_0}/r_{A_{rec}})\lambda_{em}}\lambda^1_{em},$$

hence

$$(1+z) = (1+z_+)\left[1-\left(\frac{\Delta r}{r}\right)_+\right]\left(\frac{r_{A_{rec}}}{r_{B_{rec}}}\frac{\lambda^1_{em}}{\lambda_{em}}\right).$$

Let us deal first with the third factor, which is unity for isentropic perturbations and arises from spatial variation of the specific entropy $\mathfrak{S} \equiv n_\gamma/n_B$. The Saha equation for the degree of ionization of a plasma shows that, in this expanding medium, recombination takes place at a critical temperature, or n_γ, that depends only weakly on the matter density n_B. For an estimate of $(1+z_{Gen}) \equiv [(r_{A_{rec}}/r_{B_{rec}})(\lambda^1_{em}/\lambda_{em})]$, assume that recombination takes place at the same temperature everywhere, then $\lambda^1_{em} = \lambda_{em}$. Now

$$m = \frac{4}{3}\pi\rho_{A_{rec}}r^3_{A_{rec}} = \frac{4}{3}\pi\rho_{B_{rec}}r^3_{B_{rec}},$$

so

$$\frac{r_{A_{rec}}}{r_{B_{rec}}} = \left(\frac{\rho_{B_{rec}}}{\rho_{A_{rec}}}\right)^{1/3} = \left(\frac{\mathfrak{S}_A}{\mathfrak{S}_B}\right)^{1/3} \Rightarrow z_{Gen} = \frac{1}{3}\frac{\Delta\mathfrak{S}}{\mathfrak{S}} = \frac{M}{3\mathfrak{S}}\frac{d\mathfrak{S}}{dM}\left(\frac{\Delta M}{M}\right)$$

or

$$z_{Gen} \simeq -\frac{M}{S}\frac{d\mathfrak{S}}{dM}\Delta.$$

This unknown term may be large but it cannot cancel the other terms for all observers (and thus invalidate the limits on $(\Delta\rho/\rho)_0$) since it has a different dependence on η (none). Specializing to isentropic lumps we have

$$(1+z) = (1+z_+)\left[1-\left(\frac{\Delta r}{r}\right)_+\right],$$

and substitution from (18) and (19) yields

$$z(\omega,\eta) = \frac{1}{EV}\left[S^2 + \frac{1}{2}D_k(\eta)\{S^2 - V^2 - 2V(E+V)\}\right]\Delta.$$

These lumps must have $\omega_{H_{rec}} < \eta < \omega_{H_0}$ in order that they actually straddle the photosphere. An interesting special case is $\eta = \omega$, when the lump is centred on our horizon (this is only valid for lumps larger than the horizon at recombination and smaller than the present horizon). Then

$$z = z(\omega, \omega) = \left[\frac{5E+3}{E} - \frac{6}{E}\left(\frac{1+E}{S}\right)^3 (S-\omega)\right]\Delta,$$

and

$$z \simeq \frac{\omega^2}{10}\Delta \qquad \text{(redshift)}$$

for $\omega \ll 1$,

$$z \simeq -\Delta \qquad \text{(blueshift)}$$

for $\omega \gtrsim 3$. Now if

$$\eta_0 = \omega_{H_0} \ll 1 (\Omega_0 \simeq 1), \qquad \left(\frac{\Delta\rho}{\rho}\right)_0 = \frac{3}{10}\omega_{H_0}^2 \Delta,$$

and if

$$\eta_0 = \omega_{H_0} = 3$$

say

$$(\Omega_0 \sim 0.2), \qquad \left(\frac{\Delta\rho}{\rho}\right) \simeq \frac{3}{2}\Delta,$$

$$\Rightarrow |z| \simeq \left(\frac{\omega}{\omega_{H_0}}\right)^2 g_2(\Omega_0)\left(\frac{1}{3}\frac{\Delta\rho}{\rho}\right)$$

where

$$g_2(1) = 1 \qquad g_2(0.2) \simeq 2.$$

The effect of these lumps on the last scattering surface is shown as line 2 in Fig. 4.

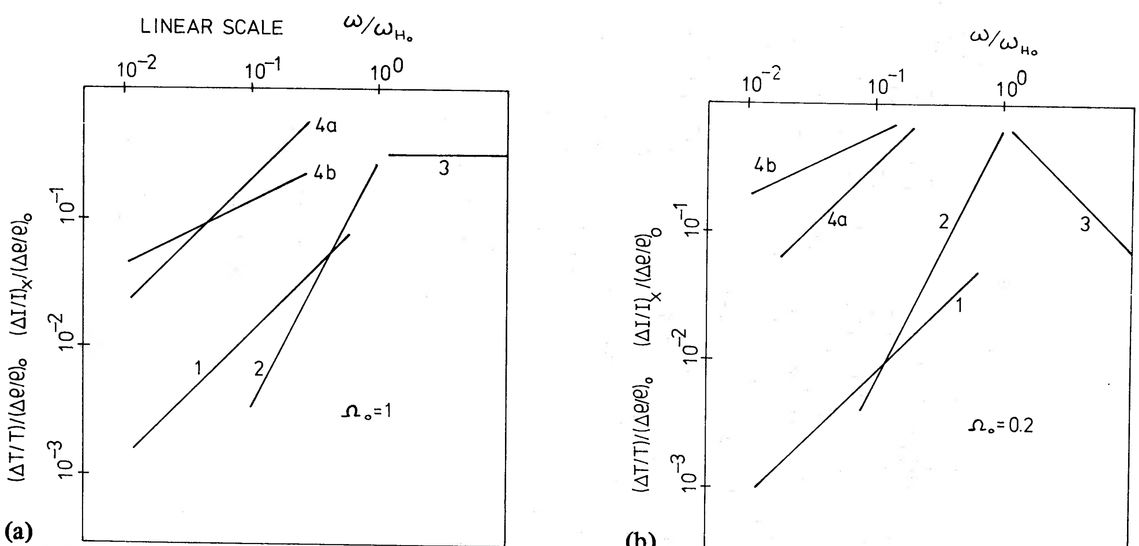

Figure 4. The strength of the different effects plotted against size of the lump for $\Omega_0 = 1$ (a) and for $\Omega_0 = 0.2$ (b). (1) The peculiar velocity effect due to a local inhomogeneity; (2) the gravitational influence of lumps on the last scattering surface; (3) quadrupole anisotropy induced by a long-wavelength perturbation; (a, b) X-ray background fluctuations.

3.4 LUMPS LARGER THAN THE PRESENT HORIZON

Previous treatments of this type of inhomogeneity have assumed that curvature is negligible on the scale of the lumps, i.e. $\omega_L \ll 1$. For example, Grishchuk & Zel'dovich perturb the Einstein–de Sitter solution to find

$$\frac{\Delta T}{T} \sim \left(\frac{\Delta \rho}{\rho}\right)_0$$

independent of ω_L. However, $\omega_L \ll 1$ implies that Ω_0 is very close to unity, since $(1/\Omega_0 - 1)^{1/2} \simeq \eta_0 = \omega_{H_0} \ll \omega_L \ll 1$, and even then, unless $\Omega_0 = 1$ exactly, there are some scales on which curvature cannot be ignored. If $\eta_0 \gtrsim 1$ and $k = -1$ then curvature is non-negligible on the scale of the horizon and this flat-space approximation breaks down completely. (If $\eta_0 \sim 1$ and $k = +1$ then we have already seen an appreciable fraction of the Universe and there are no scales $\gg$ the horizon.)

Let us calculate the anisotropy in a Swiss Cheese universe possessing a spherical inhomogeneity larger than the present horizon. The single-shell lumps used in the previous calculations would be unrealistic here, since only the untypical observer whose horizon intersects the shell would see any anisotropy at all. A more realistic lump may be constructed from nested shells as in Fig. 2. For concreteness, consider a lump having a uniform core, radius $\sim \omega_L$, surrounded by a region also of width $\sim \omega_L$ where M varies linearly with proper radius outside of which we have a uniform Friedmann background. This may be achieved with thin shells of tiny amplitude Δ_i equally spaced in ω. If the lump has total amplitude Δ then, for an observer lying in the region of varying density, $\Delta_{H_0} = (\omega_{H_0}/\omega_L)\Delta = \Sigma \Delta_i$, summed over shells within our horizon. For a more general density-profile we still expect M to vary essentially linearly over the horizon size if $\omega_{H_0} \ll \omega_L$. Let us calculate $(1+z_N) \equiv \lambda_N/\lambda_{eq}$, $(1+z_S) \equiv \lambda_S/\lambda_{eq}$, from which we may form the 'dipole' and 'quadrupole' parameters

$$D = \tfrac{1}{2}(z_s - z_N), \qquad Q = \tfrac{1}{2}(z_s + z_N)$$

for an isentropic perturbation. All the major features for the smoothed-out case can be seen in the special case in which only two vacuum shells intersect our horizon as in Fig. 2.

Let the shells be equidistant from us and have separation ω_{H_0}. Radiation crosses the lump at the epoch $\eta = \eta_* = \tfrac{1}{2}\omega_{H_0}$ and the product of the redshifts gives

$$(1+z_N) = (1+z_+)\left[1 - \left(\frac{\Delta r}{r}\right)_+\right]\Delta_{H_0},$$

$$(1+z_s) = (1+z_-)\left[1 - \left(\frac{\Delta r}{r}\right)_-\right]\Delta_{H_0},$$

but

$$z_\pm - \left(\frac{\Delta r}{r}\right)_\pm = \left[\frac{S}{E}\, q_k(\eta_*) \mp D_k(\eta_*)\right]\Delta_{H_0}$$

where

$$q_k(\eta_*) = \frac{S}{V}\left[1 - \frac{k}{2}\left(2 - \frac{3V\tau}{r}\right)\left(\frac{3V^2}{S^2} - 1\right)\right] \simeq \begin{cases} \tfrac{2}{5}\eta & \text{for } \eta \ll 1 \\ \eta \exp(-n) & \text{for } \eta \gtrsim 1 \end{cases}.$$

horizon). Then

$$z = z(\omega, \omega) = \left[\frac{5E+3}{E} - \frac{6}{E}\left(\frac{1+E}{S}\right)^3 (S-\omega)\right]\Delta,$$

and

$$z \simeq \frac{\omega^2}{10}\Delta \qquad \text{(redshift)}$$

for $\omega \ll 1$,

$$z \simeq -\Delta \qquad \text{(blueshift)}$$

for $\omega \gtrsim 3$. Now if

$$\eta_0 = \omega_{H_0} \ll 1 (\Omega_0 \simeq 1), \qquad \left(\frac{\Delta\rho}{\rho}\right)_0 = \frac{3}{10}\omega_{H_0}^2 \Delta,$$

and if

$$\eta_0 = \omega_{H_0} = 3$$

say

$$(\Omega_0 \sim 0.2), \qquad \left(\frac{\Delta\rho}{\rho}\right) \simeq \frac{3}{2}\Delta,$$

$$\Rightarrow |z| \simeq \left(\frac{\omega}{\omega_{H_0}}\right)^2 g_2(\Omega_0)\left(\frac{1}{3}\frac{\Delta\rho}{\rho}\right)$$

where

$$g_2(1) = 1 \qquad g_2(0.2) \simeq 2.$$

The effect of these lumps on the last scattering surface is shown as line 2 in Fig. 4.

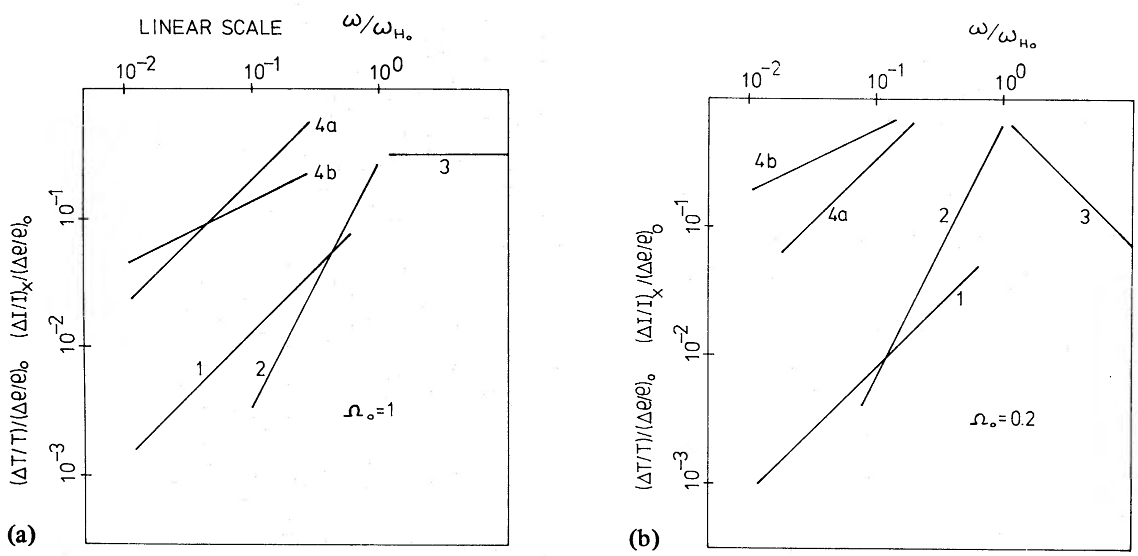

Figure 4. The strength of the different effects plotted against size of the lump for $\Omega_0 = 1$ (a) and for $\Omega_0 = 0.2$ (b). (1) The peculiar velocity effect due to a local inhomogeneity; (2) the gravitational influence of lumps on the last scattering surface; (3) quadrupole anisotropy induced by a long-wavelength perturbation; (a, b) X-ray background fluctuations.

inhomogeneity from the X-ray isotropy have been determined by Rees (1980) and in more detail by Fabian (1981).

There are two ways in which a lump can induce anisotropy in such a system.

(a) Directly – the X-ray background provides a direct probe of inhomogeneity out to $\omega \sim \omega_{\text{Hubble}}$, since we can reasonably expect X-ray production to be enhanced in regions of overdensity.

(b) Indirectly – the lumps of matter induce peculiar velocities in the observer and in the source region.

4.1 THE INDIRECT EFFECT

(1) A nearby lump induces a 24-hr anisotropy via the Compton–Getting effect – we are moving with respect to the bulk of the sources. The fluctuations in intensity will be

$$\frac{\Delta I}{I} \sim \Omega_0 \frac{\omega}{\omega_{\text{Hubble}}} \left(\frac{\Delta\rho}{\rho}\right)_0 \sim V_{\text{pec}}.$$

This must be increased by a factor ~ 3.4 relative to the analogous CMB calculation when we allow for the spectral index of the radiation, but the X-ray measurement provides at present only a ~ 1/2 per cent limit whereas the microwave anisotropy is smaller.

(2) Fabian & Warwick (1979) have argued that a lump beyond sources can produce a 12-hr effect thus: All sources (and we ourselves) fall towards the lump with different velocities and this induces shear in the source region, which itself induces a 12-hr variation through the Compton–Getting effect. This effect is most powerful for a lump just beyond the bulk of the sources; if the lump is too distant then we and the sources fall along parallel lines and the effect vanishes. This again yields $\Delta I/I \simeq (2+\alpha)v_{\text{pec}}$.

4.2 THE DIRECT EFFECT

If the X-ray source density depends on the matter density (relative to the mean) as, e.g. a power law, then a small-amplitude lump, size ω, will give to within a factor of order unity (depending on the power law)

$$\left(\frac{\Delta I}{I}\right)_{\text{lump}} \sim \frac{\omega}{\omega_{\text{Hubble}}} \frac{\Delta\rho}{\rho}.$$

In the absence of any detailed knowledge of ϵ let us assume two models:

(a) *No evolution.* The nearest lump will dominate and

$$\frac{\Delta I}{I} \sim \frac{\omega}{\omega_{\text{Hubble}}} \left(\frac{\Delta\rho}{\rho}\right)_0.$$

(b) *Evolution* has switched off the nearby sources out to z_{X}. For $\omega < \omega_{\text{Hubble}}$ there is room for $(\omega/\omega_{\text{Hubble}})^{-1}$ lumps along the line of sight. The way the effects add together on average depends on the spatial correlation of the lumps. We take as an estimate the $N^{1/2}$ contribution that we would expect for a Poisson distribution of lumps. Then

$$\frac{\Delta I}{I} \sim \left(\frac{\omega}{\omega_{\text{Hubble}}}\right)^{1/2} \frac{\Delta\rho}{\rho}$$

where

$$\frac{\Delta\rho}{\rho} \sim \left(\frac{\Delta\rho}{\rho}\right)_0 \quad \text{if } \eta \gtrsim 1,$$

and

$$\frac{\Delta\rho}{\rho} \sim \left(\frac{\eta_{\text{em}}}{\eta_0}\right)^2 \left(\frac{\Delta\rho}{\rho}\right)_0 \simeq (1+z_X)^{-1} \left(\frac{\Delta\rho}{\rho}\right)_0 \quad \text{if } \eta \ll 1.$$

The direct effect is shown as lines 4a, 4b in Fig. 4, where I have plotted $(\Delta T/T)/(\Delta\rho/\rho)_0$ and $(\Delta I/I)_X/(\Delta\rho/\rho)_0$ versus the linear dimension of the lump as a fraction of the present horizon size.

5 Observations and models

We may combine Fig. 4 with the present observational limits on $\Delta T/T$, $(\Delta I/I)_X$ on various angular scales, then put an upper limit on $\Delta\rho/\rho$. The results are shown in Fig. 3. The Fabbri *et al.* (1981) measurements at 6° and 180° appear as two points. They do not conflict with the other limits. It may turn out that these fluctuations are due to local emission, but even then the 6° point will still provide a strong upper limit to $\Delta\rho/\rho$.

We know from the galaxy correlation function that $(\Delta\rho/\rho)_{\text{Gal}} \sim 1$ on a scale of order 10 Mpc, and we see from Fig. 3 that a local lump on this scale can easily produce a significant part, if not all, of the dipole fluctuation. This does not conflict with the X-ray limits. However, if there is no source evolution then we should measure

$$\left(\frac{\Delta I}{I}\right)_X \simeq \begin{cases} 1/3 \text{ per cent if } \Omega_0 \simeq 0.2, \\ 1/10 \text{ per cent if } \Omega_0 = 1, \end{cases}$$

regardless of the size or detailed shape of the lump, since both the peculiar acceleration and the excess X-ray intensity obey an inverse-square law. Failure to detect a large X-ray fluctuation would then favour $\Omega_0 = 1$.

It is often assumed that the power spectrum of inhomogeneities was initially a power law

$$|S_k|^2 \propto k^n \Rightarrow \frac{\Delta\rho}{\rho} \propto k^{n/2+3/2}.$$

In flat space, a power law in k is a power law in linear size, surface area or volume (mass) of the lump, as these quantities are powers of one another. For perturbations to an open background, we may assume a power law in any of these quantities, these models diverging from one another on scales greater than the curvature scale. Of course there is no compelling reason why $\delta\rho/\rho$ should be a power law at all. For some values of n, a choice of argument for the power law is suggested by a simple model that displays that power law. For example, a Poisson process provides an $n = 0$ power law in (proper) mass $\Delta\rho/\rho \propto M^{-1/2}$.

For $n = -1$, $\Delta\rho/\rho \propto \omega^{-1}$ (for $\omega \lesssim 1$) and the peculiar velocity effect is the same on all scales. We can then rule out $n < -1$ models as these would produce too much peculiar velocity for large lumps, in conflict with the observed $(\Delta T/T)_{\text{dipole}}$.

If we now assume that the 6° measurement is real, and $(\Delta\rho/\rho)_{10\,\text{Mpc}} \sim 1$, we can estimate n. This normalization assumes that we have a power-law spectrum extending to small scales (~ 10 Mpc) now. This is consistent with an initial power-law spectrum only for entropy (isothermal) perturbations, since oscillation and damping will attenuate isentropic perturbations on scales less than the maximum Jeans mass. We find that, for the range of Ω_0

considered here, the results are consistent with $n = 0$. A line $\Delta\rho/\rho = (M/M_*)^{-1/2} = (\lambda/\lambda_*)^{-3/2}$ passes through the 6° point for the very reasonable values

$$\lambda_* \simeq \begin{cases} 10\ \text{Mpc if } \Omega_0 \sim 0.2, \\ 30\ \text{Mpc if } \Omega_0 = 1. \end{cases}$$

This was noticed by Peebles (1981) who showed that, for $\Omega_0 = 1$, the simple $n = 0$ model provides a prediction of $\Delta T/T(\theta)$ for large angle. Taking the Sachs & Wolfe relation

$$\frac{\Delta T}{T} \propto \omega^2 \frac{\Delta\rho}{\rho}, \quad \frac{\Delta\rho}{\rho} \propto \omega^{-3/2}, \quad \theta \propto \omega,$$

we find $\Delta T/T(\theta) \propto \theta^{1/2}$. The large-scale inhomogeneities dominate the large-scale angular fluctuations. This model predicts $(\Delta T/T)_{180°} \simeq 5(\Delta T/T)_{6°}$ which agrees well with the observed quadrupole fluctuations, considering the uncertainties. Let us now find the prediction for $\Delta T/T(\theta)$ in a low-density universe ($\Omega_0 = 0.2$).

First calculate the large angular scale $\Delta T/T$ due to large-scale $\Delta\rho/\rho$. The angle redshift relation is

$$\theta = \frac{\omega}{\sinh \omega_{H_0}} \simeq \frac{\omega}{10},$$

then

$$\omega_{6°} \sim 1, \quad \omega_{180°} \gtrsim 3\omega_{H_0} \sim 10.$$

(The intersection of a sphere equal to the horizon size with our horizon subtends a small solid angle due to the hyperbolic curvature.) The effect of a lump $\omega \sim 3\omega_{H_0}$ is drastically reduced below the flat-space estimate for two reasons: (1) the Sachs & Wolfe relation breaks down for $\omega \sim 3$ and we then have the weaker $\Delta T/T \sim \Delta\rho/\rho$, (2) The proper mass rises exponentially with ω (or θ) for $\omega \gg 1$. A power law in mass has much less power at large scales than the value predicted by the power law in angle with which it agrees for small angle.

The result of (1), (2) is that the quadrupole anisotropy is no longer dominated by the very large-scale lumps but by the effect of lumps with $\omega \sim 3$ and solid angle $\sim 1/10$, adding statistically. The hallmark of this is that at large angular scales we will have $\Delta T/T \propto \theta^{-1}$, in marked constrast to the $\Omega_0 = 1$ prediction. If the initial fluctuations are isentropic and we use $(\Delta\rho/\rho)_{10\ \text{Mpc}} \sim 1$ to normalize, then we require a larger index n (more power on small scales to overcome the damping) and again we should have $\Delta T/T(\theta)$ decreasing at large scales.

If the $\Delta T/T \propto \theta^{1/2}$ trend suggested by the Fabbri *et al.* measurement is confirmed, and is truly extragalactic, this would be very difficult to reconcile with a power law extending to large masses in a low-density universe.

A further departure from the $\theta^{1/2}$ prediction is expected at small θ, since the Sachs & Wolfe effect is only dominant for $\omega > \omega_{H_{\text{dec}}}$ or $\theta \gtrsim 3°\sqrt{\Omega_0}$. We expect a larger $\Delta T/T$ for a range of angles (perhaps one decade) below the horizon size at last scattering, down to the scale at which these effects are attenuated by the finite width of the photosphere.

Even if a power-law spectrum is observed over a wide range of scales, there may be an upper limit beyond which the power law breaks down. The quadrupole anisotropy limit (measurement) still provides a constraint on the amplitude of inhomogeneities on very large scales (under the usual statistical assumption that we are not privileged observers).

If Ω_0 is very close to unity, then this amplitude limit is $\sim (\Delta T/T)_{180°} \sim 3 \times 10^{-4}$ on all scales up to the curvature scale. In a low-density universe, $\Delta\rho/\rho \leqslant (\omega_L/\omega_{H_0})(\Delta T/T)_{180°}$, a much weaker constraint. For instance, this does not preclude $\Delta\rho/\rho \sim 1$ on a scale $\omega \gtrsim 1/(\Delta T/T)_{180°}(\omega_{H_0}) \sim 3000\, \omega_{H_0}$.

6 Conclusions

We have created a model lumpy universe in which the density and density contrast are adjustable parameters, and have compared the predicted fluctuations in background radiation fields with current observations. From the upper limits on fluctuations in the CMB we can rule out a power-law spectrum of inhomogeneities with index $n < -1$. Differences between models with different densities do not at present allow us to rule out some values of Ω_0. Two detectable quantities that are potentially sensitive to Ω_0 are the ratio of the amplitude of X-ray and CMB dipole fluctuations, and the spectrum of fluctuations in the CMB at large angular scale. The $\Delta T/T \propto \theta^{1/2}$ spectrum suggested by recent observations at 6° and 180° favours a high-density model with a white noise spectrum of perturbation. Further observations of $\Delta T/T$ on angular scales $\gtrsim 1°$ would be of greater value.

Acknowledgments

I thank M. J. Rees and A. C. Fabian for helpful discussions and acknowledge the support of an SRC studentship.

References

Anile, A. M. & Motta, S., 1976. *Astrophys. J.,* **207**, 685.
Boughn, S. P., Cheng, E. S. & Wilkinson, D. T., 1981. *Astrophys. J.,* **243**, L113.
Dyer, C. C., 1976. *Mon. Not. R. astr. Soc.,* **175**, 429.
Einstein, A. & Straus, E. G., 1945. *Rev. Mod. Phys.,* **17**, 120; **18**, 148.
Fabbri, R. Guidi, I., Melchiorri, F. & Natale, V., 1980. *Phys. Rev. Lett.,* **44**, 1563.
Fabbri, R., Guidi, I., Melchiorri, F. & Natale, V., 1981. Preprint.
Fabian, A. C., 1981. *Ann. N. Y. Acad Sci.,* in press.
Fabian, A. C. & Warwick, R. S., 1979. *Nature,* **280**, 39.
Fabian, A. C., Warwick, R. S. & Pye, J. P., 1980. *Physica Scripta,* **21**, 650.
Grischuk, L. P. & Zel'dovich, Ya. B., 1978. *Astr. Zh.,* **55**, 209.
Kantowski, R., 1969. *Astrophys. J.,* **155**, 90.
Misner, C. W., Thorne, K. S. & Wheeler, J. A., 1973. *Gravitation,* p. 588, W. H. Freeman, San Francisco.
Peebles, P. J. E., 1976. *Astrophys. J.,* **205**, 318.
Peebles, P. J. E., 1981. *Astrophys. J.,* **243**, L113.
Rees, M. J., 1980. *IAU Symp. 92,* 207.
Rees, M. J. & Sciama, D. W., 1968. *Nature,* **217**, 511.
Sachs, R. K. & Wolfe, A. M., 1967. *Astrophys. J.,* **147**, 73.
Smoot, G. F., 1980. *Physica Scripta,* **21**, 619.
Smoot, G. F., Gorenstein, M. V. & Muller, R. A., 1977. *Phys. Rev. Lett.,* **39**, 898.
White, S. D. M., 1980. *Physica Scripta,* **21**, 619.